SUPPLEMENTAL MATERIAL

Yang et al., https://doi.org/10.1084/jem.20161900

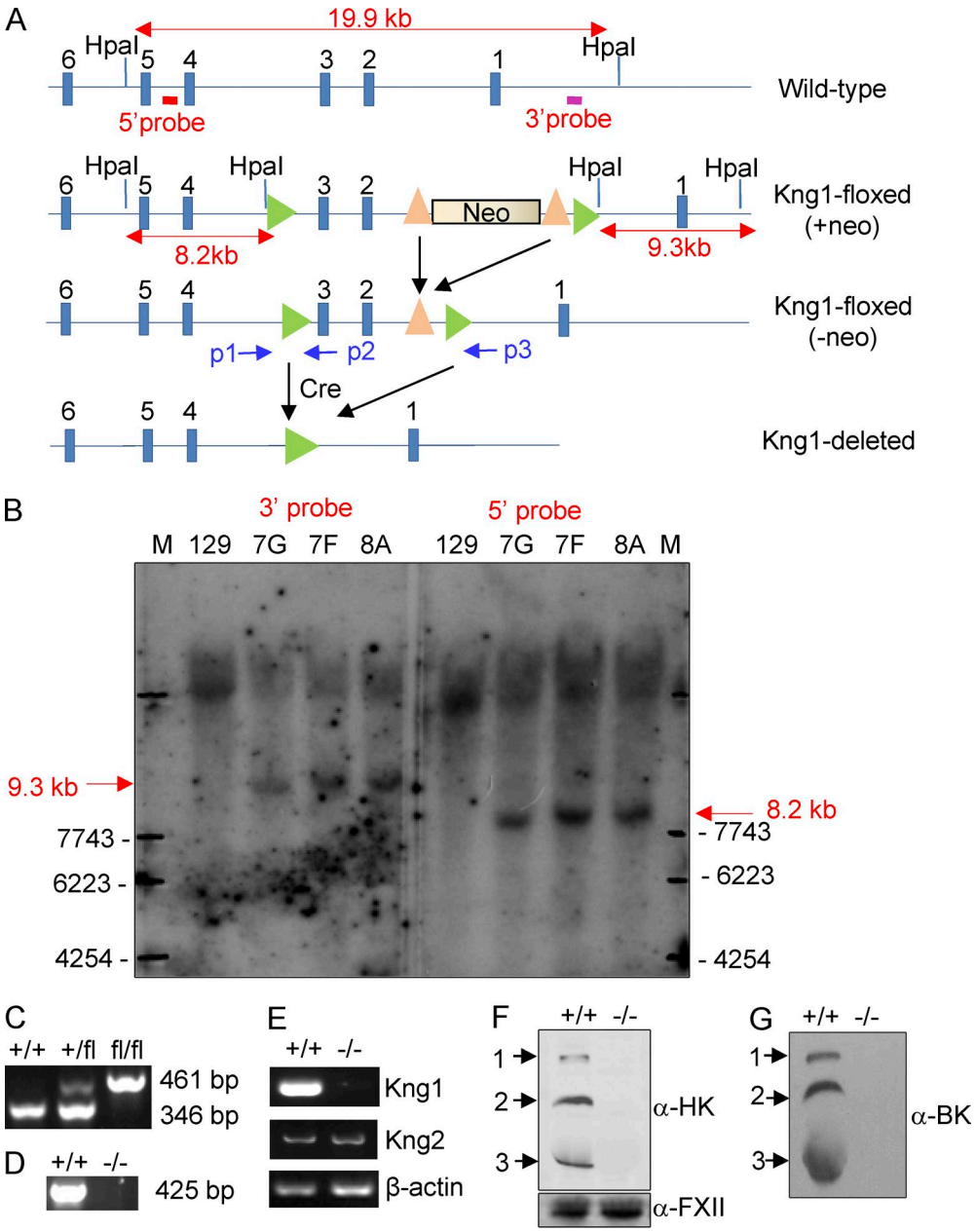

Figure S1. **Generation and characterization of *Kng1*$^{-/-}$ mice.** (A) A schematic diagram of mouse *Kng1* gene deletion. A targeting vector in which the *Kng1* floxed allele was created by inserting the loxP-PGK-Neo-loxP cassette into exons 2 and 3. Kng1-floxed mice were then mated with CMV-Cre (Cre) mice to generate whole-body knockouts. (B) Southern blot showing the gene-modified stem cells (7G, 7F, and 8A) positive for containing the modification cassette. (C) Genotyping of tail DNA from *Kng1*$^{fl/fl}$, *Kng1*$^{+/fl}$, and *Kng1*$^{+/+}$ mice. PCR using primer 1 (p1) and primer 2 (p2) (shown in A) produced a 461-bp product for the *Kng1*-floxed allele and a 346-bp product for the WT allele. (D) Genotyping of tail DNA from WT mice and *Kng1*$^{-/-}$ mice. PCR using primer 1 (p1) and primer 3 (p3) (shown in A) yielded a 425-bp product for the *Kng1*-deleted allele and no product for the WT allele. (E) Absence of expression of Kng1 mRNA in the liver of *Kng1*$^{-/-}$ mice. Total RNA was isolated from the liver of WT mice and *Kng1*$^{-/-}$ mice, and the expression of Kng1 and Kng2 mRNA was measured by RT-PCR using β-actin mRNA as the loading control. (F) Absence of expression of the HK antigen in plasma from *Kng1*$^{-/-}$ mice. Mouse plasma from WT and *Kng1*$^{-/-}$ mice was immunoblotted with an anti-HK antibody. The arrows (1, 2, 3) indicate the three mouse kininogen species. Immunoblotting with an anti-FXII antibody served as the loading control. (G) Absence of expression of the HK antigen in plasma from *Kng1*$^{-/-}$ mice shown by immunoblotting using anti-BK antibody. Mouse plasma from WT and *Kng1*$^{-/-}$ mice was immunoblotted with anti-BK antibody. The arrows (1, 2, 3) indicate the three mouse kininogen species.

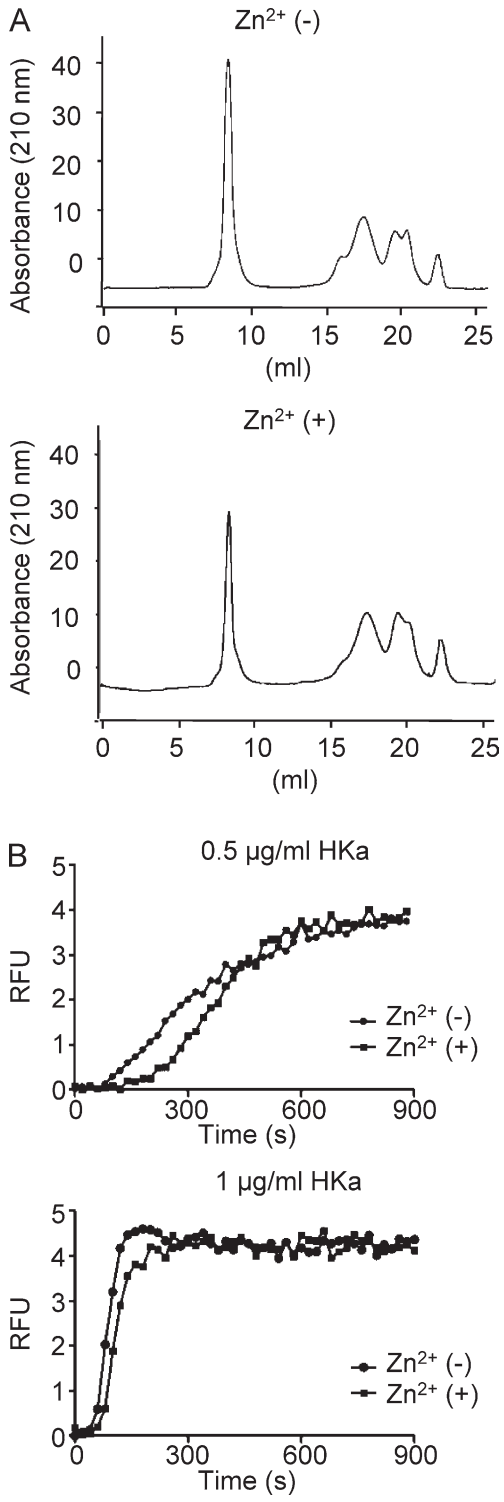

Figure S2. **HK interaction with LPS is not dependent of Zn^{2+}.** (A) FPLC of Superdex-200 elution profiles of HK incubated with LPS. LPS (250 µg/ml) was incubated with HK (50 µg/ml) at 37°C for 60 min in a final volume of 200 µl in the presence or absence of 50 µM $ZnCl_2$. Samples were then loaded onto the column, which was equilibrated with PBS and which was used as the elution buffer with a flow rate of 0.6 ml/min. The absorbance was monitored at 210 nm. Data are representative of two independent experiments. (B) BODIPY FL–LPS at 50 ng/ml was suspended in 100 µl of PBS. After the addition of human HKa at the indicated concentrations in the presence and the absence of 50 µM $ZnCl_2$, the real-time change in BODIPY FL–LPS fluorescence upon transition from the aggregated LPS state was recorded in 20-s intervals. Data are representative of two independent experiments. RFU, relative fluorescence units.

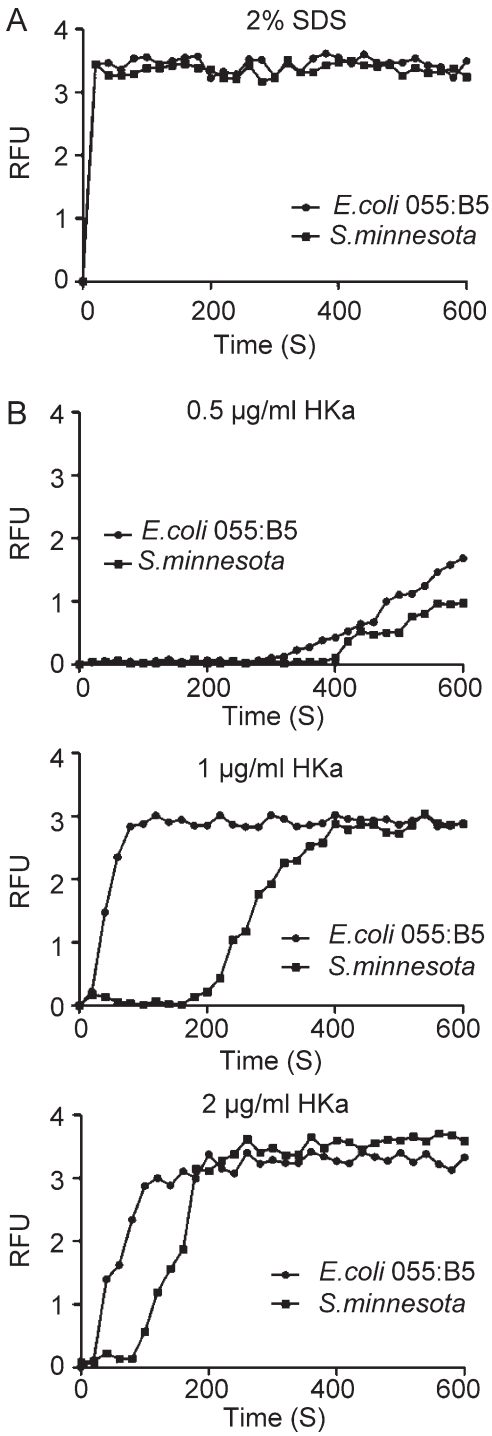

Figure S3. **Disaggregation of *E. coli* 055:B5 LPS and *S. minnesota* LPS by HKa.** (A) 50 ng/ml BODIPY FL–labeled *E. coli* 055:B5 LPS or *S. minnesota* LPS in 100 µl PBS was incubated with 2% SDS, and the real-time change in BODIPY FL-LPS fluorescence upon transition from the aggregated LPS state was recorded. (B) BODIPY FL–labeled *E. coli* 055:B5 LPS or *S. minnesota* LPS (50 ng/ml) was suspended in 100 µl PBS. After the addition of HKa at the indicated concentrations, the real-time change in BODIPY FL–LPS fluorescence upon transition from the aggregated LPS state was recorded. Data are representative of two independent experiments. RFU, relative fluorescence units.

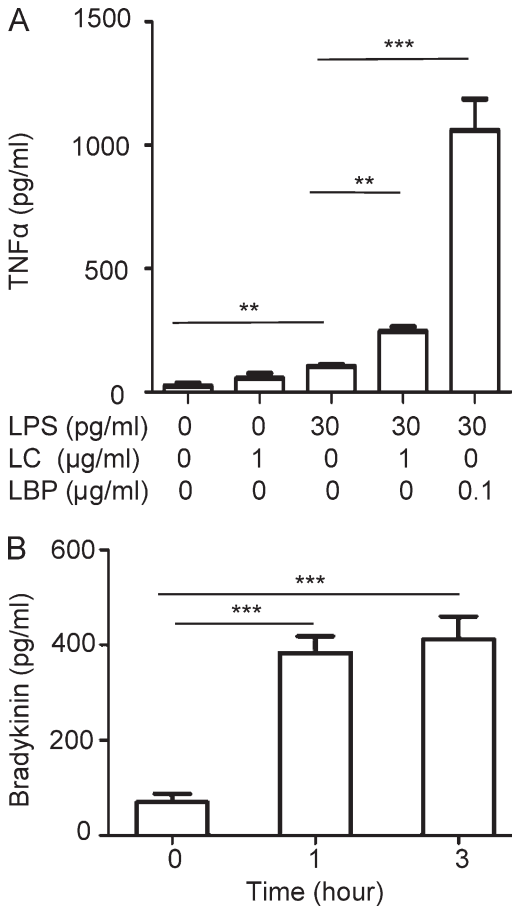

Figure S4. **LC enhances LPS-stimulated TNF production.** (A) As indicated, Raw 264.7 cells were incubated with LC or LBP in the presence or absence of LPS in serum-free DMEM medium at 37°C for 6 h. The concentration of TNF in culture supernatants was determined by ELISA. Data were analyzed using an ANOVA. **, $P < 0.01$; ***, $P < 0.001$. Data are representative of two independent experiments and expressed as mean ± SEM. (B) WT mice were challenged with 5 mg/kg of LPS (i.p.) and blood was collected at the indicated time periods. The BK concentration in plasma was measured using an ELISA kit. Data were analyzed using an ANOVA. ***, $P < 0.001$. Data are representative of two independent experiments expressed as mean ± SEM.

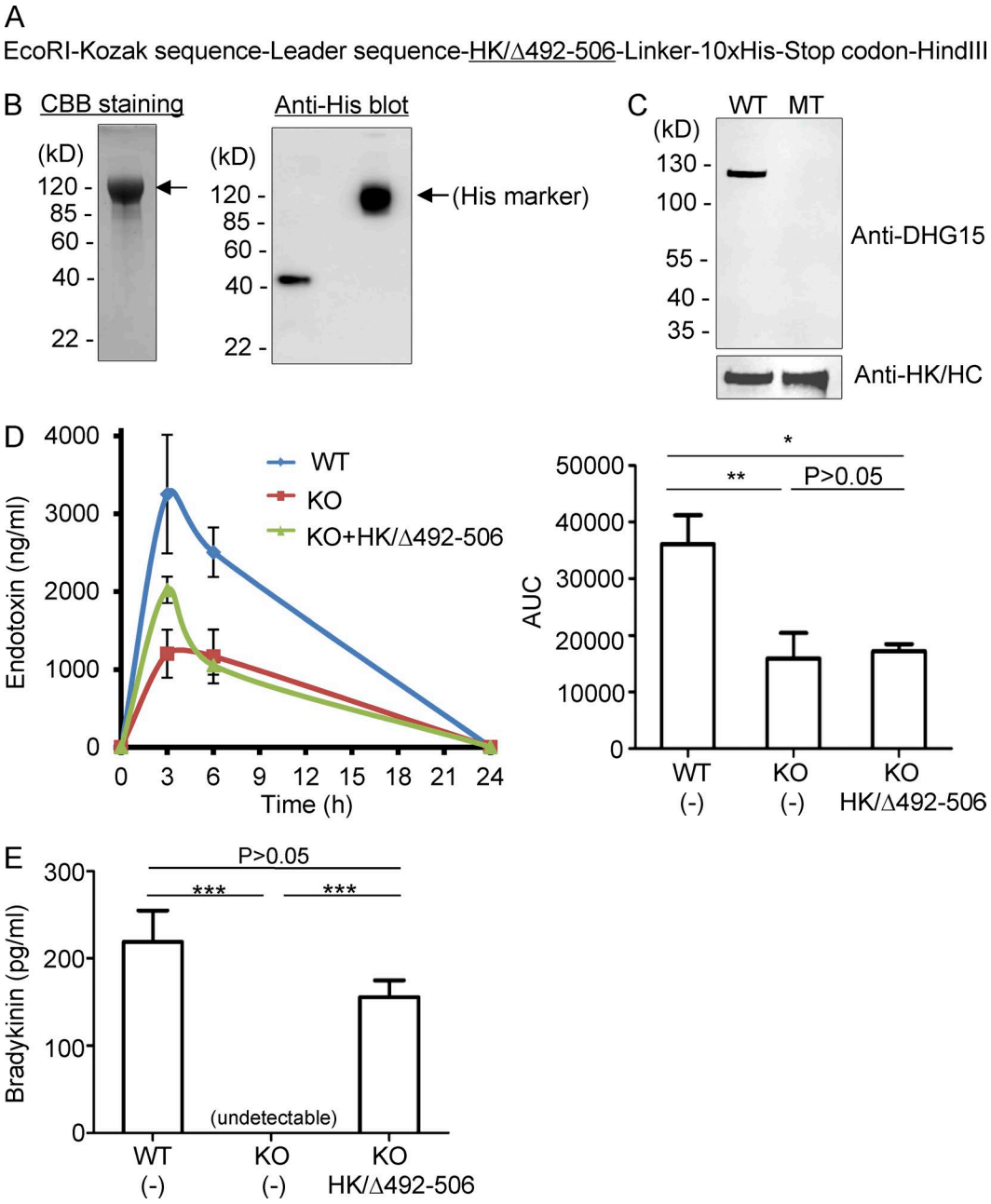

Figure S5. **Reconstitution of *Kng1*$^{-/-}$ mice with a mutant HK lacking the DHG15 region fails to recover plasma LPS levels.** (A) Cloning strategy for the generation of the recombinant HK protein lacking the DHG15 region (HK/Δ492-506). (B) Coomassie brilliant blue (CBB) staining and anti-His antibody immunoblotting of the HK/Δ492-506 protein (indicated by the arrow) after electrophoresis under reducing conditions on SDS-PAGE gels. (C) Immunoblotting of HK and HK/Δ492-506 using an anti-DHG15 antibody (top) and an anti–HK-HC antibody (bottom). (D) WT mice, *Kng1*$^{-/-}$ mice, and *Kng1*$^{-/-}$ mice reconstituted with HK/Δ492-506 (n = 6) were challenged by LPS as described in the legend for Fig. 4 B, followed by measurement of circulating LPS levels (left) and a calculation of the area under the curve (AUC) (right). Data were analyzed using an ANOVA and are representative of two independent experiments (mean ± SEM). *, P < 0.05; **, P < 0.01. (E) The levels of BK in plasma in (D) were measured by ELISA. Data were analyzed using an ANOVA. ***, P < 0.001. Data are representative of two independent experiments and expressed as mean ± SEM.